Received: 28 July 2017 | Revised: 4 September 2017 | Accepted: 7 September 2017

DOI: 10.1002/aoc.4125

FULL PAPER

WILEY Applied Organometallic Chemistry

DNA/BSA binding interactions and VHPO mimicking potential of vanadium(IV) complexes: Synthesis, structural characterization and DFT studies

M.A. Neelakantan | Chithiraivel Balakrishnan | V. Selvarani | M. Theetharappan

Chemistry Research Centre, National Engineering College, K.R. Nagar, Kovilpatti, 628 503 Thoothukudi District, Tamil Nadu, India

Correspondence
Neelakantan Mallanpillai Ananthakrishnan Nair, Chemistry Research Centre, National Engineering College, K.R. Nagar, Kovilpatti 628 503, Thoothukudi District, Tamil Nadu, India.
Email: drmaneelakantan@gmail.com; maneels@rediffmail.com

Funding information
Science and Engineering Research Board (SERB), Department of Science and Technology, India, Grant/Award Number: EMR-II/2014/000081

Vanadium(IV) Schiff base complexes (VOL^1-VOL^3) were synthesized and characterized by elemental analysis, various spectral methods and single crystal XRD studies. Structural analysis of VOL^2 reveals that the central vanadium ion in the complex is six coordinate with distorted octahedral geometry. Density functional theory (DFT) and time dependent (TD-DFT) studies were used to understand the electronic transitions observed in the complexes in UV–Vis spectra. The electrochemical behavior of the complexes was investigated in acetonitrile medium exhibit quasi-reversible one electron transfer. The DNA and BSA protein binding interaction of vanadium complexes has been explored by UV–Vis and fluorescence spectral methods and viscosity measurements reveal that the complexes interact with CT-DNA through intercalation mode and follows the order $VOL^1 < VOL^3 < VOL^2$. The complexes exhibit binding interactions with BSA protein. The complexes act as chemical nuclease and cleave DNA in the presence of H_2O_2. The 2,2-diphenyl-1-picrylhydrazyl (DPPH) assay was used to evaluate the radical scavenging activity demonstrate the antioxidant property of the complexes. The antimicrobial activity was screened for several microorganisms, *Staphylococcus aureus, Bacillus subtilis, Pseudomonas aeruginosa, Escherichia coli*. The mimicking of vanadium haloperoxidase was investigated by the bromination of the organic substrate phenol red by vanadium complexes in the presence of bromide and H_2O_2.

KEYWORDS
vanadium(IV) complexes, DNA binding and cleavage, oxidative bromination of phenol red, Schiff bases

1 | INTRODUCTION

Metal complexes due to their tunable geometry, intense metal to ligand charge transfer bands, versatile redox and propensity for binding to biomolecules are useful probes for studying the drug-DNA interactions.[1] Metal complexes interact with DNA through non-covalent interactions (intercalation and groove-binding) or/and electrostatic.[2] Schiff base metal complexes containing planar aromatic groups exhibit DNA interactions via intercalative mode and have potential antiproliferative abilities.[3] The primary intracellular target for drugs is DNA base pairs, which can damage the cells and prevent the replication, resulting in cell death.[4] Thus, the DNA-metal complex interaction studies are important for the design and development of novel drugs in medicine

without any side effects.[5] Metal complexes are capable of acting as artificial nucleases and cleave DNA, thus leads to develop new chemotherapeutic agents.

Vanadium in the form of $Na^+H_2VO_4^-$ is the second-most abundant transition metal in seawater.[6] It is an essential trace element for some living organisms and possibly essential for normal human health. *In vivo*, vanadium acts as metal cation or as phosphate analogue depending upon the oxidation state of the metal.[7] In protein, DNA and RNA vanadium ions play a role as counter ions.[2,8] Vanadium dependent haloperoxidase enzymes have been identified in marine algae,[9] lichens[10] and fungi.[11] In algal bromoperoxidase and in certain prokaryotic nitrogenases, vanadium acts as a cofactor. Vanadium haloperoxidase catalyzes many organic compounds by oxidative halogenation in the presence of halide ions and hydrogen peroxide.[12] Biosynthesis of many natural products is catalyzed by vanadium bromoperoxidase.[13] The presence of vanadium in vanadium haloperoxidase, and the insulin-mimic activity,[14] and potential anticancer activity[14] of some vanadium complexes created interest towards the studies on coordination chemistry of vanadium. In vanadium haloperoxidase enzyme the histidine component is covalently bonded to a vanadate moiety.[15] Thus the development of vanadium complexes containing oxygen and nitrogen ligation sites is important.[16]

The hydroxyl-substituted Schiff bases have drawn considerable attention owing to their effective coordination with metal ions and their pharmacological properties.[17–20] The propargyl group containing compounds play a significant role in neuroprotection and having exclusive inhibitory properties towards the flavin-linked oxidases.[21] In view of all these facts, we synthesized three vanadium(IV) Schiff base complexesand characterized by various spectral methods and single crystal XRD analysis. The DNA binding and cleavage activities of the complexes were studied by different spectral techniques. The antioxidant and antimicrobial activities of metal complexes were also investigated. The catalytic potential of these complexes were evaluated by the oxidative bromination of phenol red to bromophenol blue.

2 | EXPERIMENTAL

2.1 | Materials and methods

2,4-dihydroxybenzaldehyde, 3-bromopropyne, 1,2-diaminopropane, 1,3-diaminopropane, ethylenediamine, vanadyl sulphate, potassium iodide, potassium bicarbonate and triethylamine were procured from Aldrich. Microanalyses were done with an Elemental Vario EL III CHNOS elemental analyzer. Conductance measurements were performed using a Metrohm 712 conductometer. Magnetic measurements were made on powdered samples at 25 °C using Guoy balance. FT-IR spectra were recorded on Shimadzu 8400 IR Spectrophotometer using KBr pellets. UV–Visible spectra of the compounds were recorded on Shimadzu 2450 UV–Vis spectrophotometer. Fluorescence spectra were performed on Jasco FP-8300 fluorescence Spectrofluorometer. Cyclic voltammetry studies were performing using CHI620E spectroelectrochemical workstation. The working electrode was glassy carbon; platinum wire was used as the auxiliary electrode, Ag/AgCl as reference electrode. Electrochemical experiments were done at room temperature using buffer solution of vanadium complexes with 5% DMSO containing tetrabutylammonium perchlorate (TBAP) as the supporting electrolyte.

2.2 | Synthesis of vanadium Schiff base complexes

Synthesis of Schiff bases (L^1-L^3) are reported in our previous paper.[3] The Schiff base vanadium complexes (VOL^1-VOL^3) were synthesized by addition of methanolic solution of respective Schiff bases (L^1-L^3) (10 mmol) with aqueous solution of vanadium sulfate (10 mmol) followed by Et_3N (20 mmol) solution. The reaction mixture was refluxed for 5 h and the obtained green precipitate was filtered and washed with ethanol (Scheme 1). After that this dried compound was dissolved in DMSO and layered by methanol for crystallization. Dark green color block shaped crystal of VOL^2 was obtained after one week time.

VOL^1: Yield: 82%. M.p.: 240 °C. Anal. Calc. for $C_{23}H_{20}N_2O_5V$: C, 60.67; H, 4.43; N, 6.15; Found: C, 60.35; H, 4.85; N, 6.35 (%). FT-IR (KBr disk, cm^{-1}) (Selected bands): 2108 terminal υ(C ≡ CH), 1596 υ(C = N), 879 υ(V = O). UV–Vis (λ_{max}/nm): 459, 575. μ_{eff}: 1.73 B.M. Λm (Ω^{-1} mol^{-1} cm^2): 8.9

VOL^2: Yield: 85%. M.p.: 271 °C. Anal. Calc. for $C_{23}H_{20}N_2O_5V$: C, 60.67; H, 4.43; N, 6.15; Found: C, 60.42; H, 4.67; N, 6.13.26 (%). FT-IR (KBr disk, cm^{-1}) (Selected bands): 2103 terminal υ(C ≡ CH), 1599 υ(CH = N), 904 υ(V = O). UV–Vis (λ_{max}/nm): 454, 570.μ_{eff}: 1.78 B.M. Λm (Ω^{-1} mol^{-1} cm^2): 10.7

VOL^3: Yield: 84%. M.p.: 269 °C. Anal. Calc. for $C_{22}H_{18}N_2O_5V$: C, 59.87; H, 4.11; N, 6.35; Found: C, 59.86; H, 4.10; N, 6.33 (%). FT-IR (KBr disk, cm^{-1}) (Selected bands): 2106 terminal υ(C ≡ CH), 1601 υ(CH = N), 896 υ(V = O). UV–Vis (λ_{max}/nm): 416, 583.μ_{eff}: 1.75 B.M. Λm (Ω^{-1} mol^{-1} cm^2): 7.1

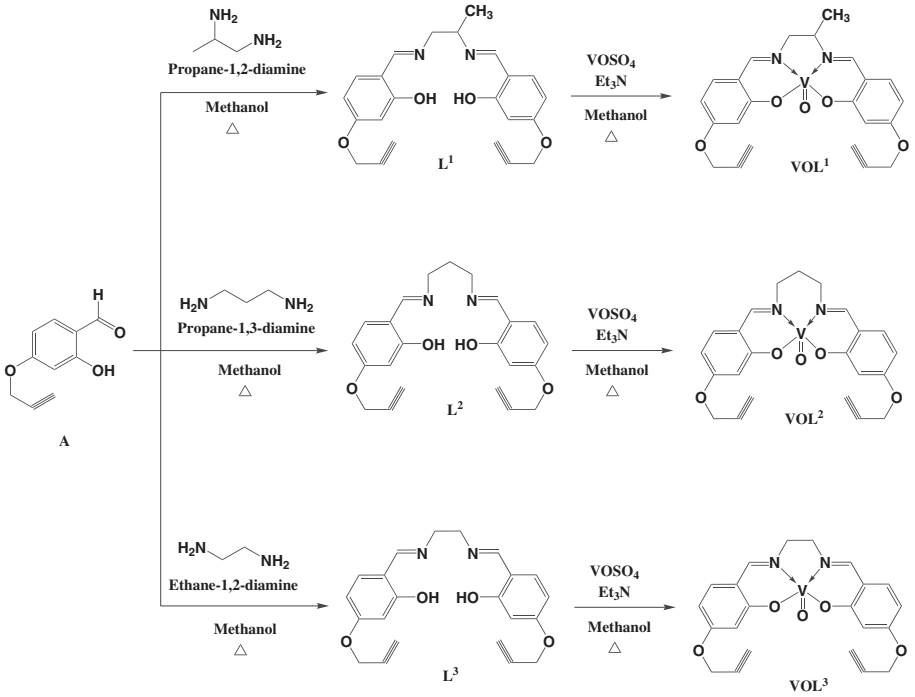

SCHEME 1 Synthesis of Schiff bases (L^1-L^3) and vanadium complexes (VOL^1-VOL^3)

2.3 | Single crystal XRD analysis

X-ray diffraction details of vanadium complex (VOL^2) were collected on a Bruker SMART APEX II diffractometer equipped with graphite monochromated (Mo*Kα* radiation (λ = 0.71073 Å) at 293(2) K.[22] The structure was solved by conventional direct methods, as implemented in SHELXS-97 program. E-Map calculated for the best phase generated by the SHELXS program revealed the positions of all the non-hydrogen atoms and these were refined by a full-matrix least squares refinement procedure using SHELXL-97.[23] The positions of all the hydrogen atoms were fixed geometrically. The hydrogen atoms were included in the refinement by allowing them to ride on the corresponding carrier atoms. The refinement converged to a final *R* factor of 0.0542.

2.4 | DFT studies

The DFT calculations were performed using Gaussian 09 package[24] at B3LYP level.[25] All the elements except vanadium were assigned the 6-311G(d,p) basis set. Lanl2dz basis set with effective core potential was used for the vanadium atoms.[26] The vibrational frequency calculations were carried out to ensure that the optimized geometries correspond to the local minima and there are only positive Eigen values.

2.5 | Biological studies

2.5.1 | Absorption method

DNA binding studies were done in Tris–HCl/NaCl buffer (5 mMTris–HCl, 50 mM NaCl, pH 7.2) containing 5% acetonitrile. DNA gave the ratio of absorbance at 260 and 280 nm, (260/280 = 1.86), demonstrating that the DNA was adequately free of protein.[27] The DNA concentration of per nucleotide was calculated from the absorption intensity at 260 nm (ε = 6600 M^{-1} cm^{-1}).[28] The UV–Visible spectral titrations were performed in buffer using a fixed concentration of the vanadium complexes (40 μM) in the range of 200–400 nm to increments of DNA. Vanadium complex-DNA solutions were allowed to incubate for 1 h before the spectra were recorded. The intrinsic association constant, K_b was determined by the following equation,

$$\frac{[DNA]}{(\varepsilon_a - \varepsilon_f)} = \frac{[DNA]}{(\varepsilon_b - \varepsilon_f)} + \frac{1}{K_b(\varepsilon_b - \varepsilon_f)}$$

where, ε_a, ε_f and ε_b are the extinction coefficient of the apparent, free and bound metal complex, respectively. The association constant (K_b) determined from the ratio of slope to intercept from the plot of [DNA]/(ε_a – ε_f) vs. [DNA].

2.5.2 | Emission method

The binding interaction of metal complex with CT-DNA was further evaluated using emission spectral techniques. The emission intensities of ethidium bromide (EB) bound DNA was measured at 602 nm with an excitation wavelength of 580 nm in the absence and presence of vanadium complex (0.0–100 μM) in Tris–HCl buffer (5mMTris–HCl, pH 7.2). The emission intensity of EB bound DNA was measured, which is used to find out the binding ability of metal complexes. Using classical Stern-Volmer equation,

$$F_0/F = 1 + K_{sv}[Q] = 1 + K_q\tau[Q]$$

where F_0 and F is the emission intensity in the absence presence of quencher, K_{sv} is the Stern-Volmer quenching constant, K_q is DNA quenching rate constant and τ is DNA average lifetime without quencher, which is equal to 10^{-8} s for bio-macromolecules,[29] the quenching constant (K_{sv}) value is obtained as a slope from the plot of F_0/F vs. [Q]. The K_b and n can be calculated from the equation,[30]

$$\log(F_0 - F)/F = \log K_b + n\log[Q]$$

where K_b is the binding constant and n is the number of binding sites in DNA base pairs. The plots of $\log[(F_0 - F)/F]$ vs. log[Q].

2.5.3 | DNA cleavage experiment

DNA cleavage ability of vanadium complexes (VOL^1-VOL^3) was done using supercoiled (SC) pUC19 DNA in 50 mM Tris–HCl/10 mM NaCl buffer. Stock solutions of metal complexes were prepared in acetonitrile and the pH was adjusted to 7–8 by addition of base. The reactions were carried out incubating DNA (20 μM) at 36 ± 0.1 °C in the presence/absence of metal complexes (40 μM) for 1 h. After incubation, the reaction mixture was loaded on 0.8% agarose gel for electrophoresis in TBE buffer (50 mM Tris base, 25 mM boric acid, 2 mM EDTA) at 100 V for 1 h. Finally the gel was photographed under UV light by LARK gel documentation system.

2.5.4 | Thermal denaturation study

DNA helix melting studies were employed by using Shimadzu-2450 spectrophotometer equipped with digital temperature controller. The temperature was gradually increased at a rate of 5 °C min^{-1} and the absorbance of CT-DNA (100 μM) was measured at 260 nm in the absence/presence of metal complexes (20 μM). The melting temperature (T_m) values were determined from the plot of relative absorbance ($A/A_{30°}$) vs. temperature, where A is the observed absorbance and A_{30} is the absorbance at 30 °C.

2.5.5 | Viscosity experiments

Viscosity experiments were carried out using Ostwald type viscometer at 30.0 ± 0.1 °C in a thermostatic water bath. DNA (100 μM) were titrated with vanadium complex (0.0-100 μM), examined the difference in the viscosity and the flow time was measured with a digital stopwatch. The specific viscosity values were calculated using the equation, $\eta = (t–t_o)/t_o$, where t_o and t is the total flow time for the buffer and for DNA in the presence and absence of the metal complex, respectively. The data are obtainable as $(\eta - \eta_o)^{1/3}$ vs. binding ratio, where η is viscosity of DNA in the presence of metal complexes and η_o is viscosity of DNA alone.

2.6 | Protein binding studies

The protein binding studies of vanadium complexes were performed by using fluorescence spectral method. The protein stock solution was prepared in 50 mM phosphate buffer (pH 7.2) and stored in the dark at 4 °C for further use. A solution of BSA (1.0×10^{-6} M) was titrated with different concentrations of vanadium complex (0.0–50 μM). Fluorescence spectra of the samples were recorded in the wavelength range of 290–450 nm upon excitation at 280 nm. Synchronous fluorescence spectra were also recorded with the same concentration of BSA and the complex corresponding to the Δλ values (difference between the excitation and emission wavelengths of BSA), 15 and 60 nm.

2.7 | Antioxidant activity

DPPH assay is used for the measurement of antioxidant activity of the vanadium complexes. 0.001 M concentration of the Schiff base (L^1-L^3) or VOL^1-VOL^3 solution is added to 0.001 M DPPH. The reaction mixture kept at room temperature for 30 minutes in dark. The spectrophotometric measurements were done at 517 nm. For positive control, ascorbic acid is used. These measurements are run in triplicate. The % of scavenging activity inhibition is calculated,

$$\text{Scavenging activity } (\%) = [(A_0–A)/A_0]\times 100$$

Where A_0 is the absorbance of $DPPH^•$ without the vanadium complex and A is the absorbance of DPPH in the presence of complex. The IC_{50} value is the concentration of the antioxidant required to scavenge 50% $DPPH^•$ and is calculated from the inhibition curve.

2.8 | Antibacterial assay

The microbial activity of the synthesized compounds against bacterial strains *Staphylococcus aureus, Bacillus subtilis, Pseudomonas aeruginosa, Escherichia coli* was determined by disc diffusion method in Mueller-Hinton Agar.[31] The *in vitro* antibacterial activity was carried out against 24 h cultures of bacterial strains. Stock solutions of test compounds (0.001 M) were prepared in 95% aqueous medium containing 5% DMSO. Sterilized agar media (20 ml) was poured into each pre-sterilized Petri dish. Solidification is allowed by placing the plates in an incubator at 37 °C for 1 h. 24 h culture suspension was poured and neatly swabbed with the pre-sterilized cotton swabs. 5 mm diameter of paper disk soaked in 20 μL of 0.001 M compounds was placed on the inoculated plates and allowed to dry for 15 min. These dishes were transferred to an incubator maintained at 37°C for 24 h. The microbial activity was measured from the diameter of the clear zone appeared around the papers in each plate. Experiments were triplicates and standard deviation was calculated.

3 | RESULT AND DISCUSSION

3.1 | Synthesis of vanadium Schiff base complexes

The synthesis of Schiff bases (L^1-L^3) were reported in our earlier work.[3] All the vanadium complexes (VOL^1-VOL^3) were synthesized by adding methanolic solution of respective Schiff bases (L^1-L^3) (10 mmol) to aqueous solution of vanadium sulfate (10 mmol) followed by Et_3N (20 mmol) solution. The reaction mixture was refluxed for 5 h and the obtained green precipitate was filtered and washed with ethanol (Scheme 1). Crystal of VOL^2 suitable for X-ray analysis was obtained by dissolving the complex in DMSO and layered by methanol. Dark green color block shaped crystal of VOL^2 was obtained after one week time.

3.2 | Crystal structure description

The asymmetric unit of brown VOL^2 complex consists of one independent molecule (Figure 1). The compound crystallizes in monoclinic system with space group $P2_1/c$. The V(IV) center of VOL^2 complex is hexacoordinated and is present in a distorted octahedral VO4N2 coordination with the basal plane by the Schiff base molecule through O1, O3, N1, N3 atoms and O6 of the solvent DMSO molecule. Vanadyl oxygen O5 occupies the axial position, which forms angle between 94.84(17)° to 105.19(17)° range with the basal plane defined previously. The crystallographic data and observed intra and intermolecular interactions are given in Table 1 and S1. From the crystal packing of VOL^2, it is clear that C–H···O intermolecular interactions stabilize the metal complex (Figure S1). Atom C24 acts as a donor to $O1^i$ and atom C25 acts as a donor to $O3^i$, generating $R_2^2(8)$ graph set motif. Both the aromatic rings are planar, with a maximum deviation of 0.016(3) Å in the ring (C15-C20). The dihedral angle between the aromatic rings is 53.46(2)°. The sum of bond

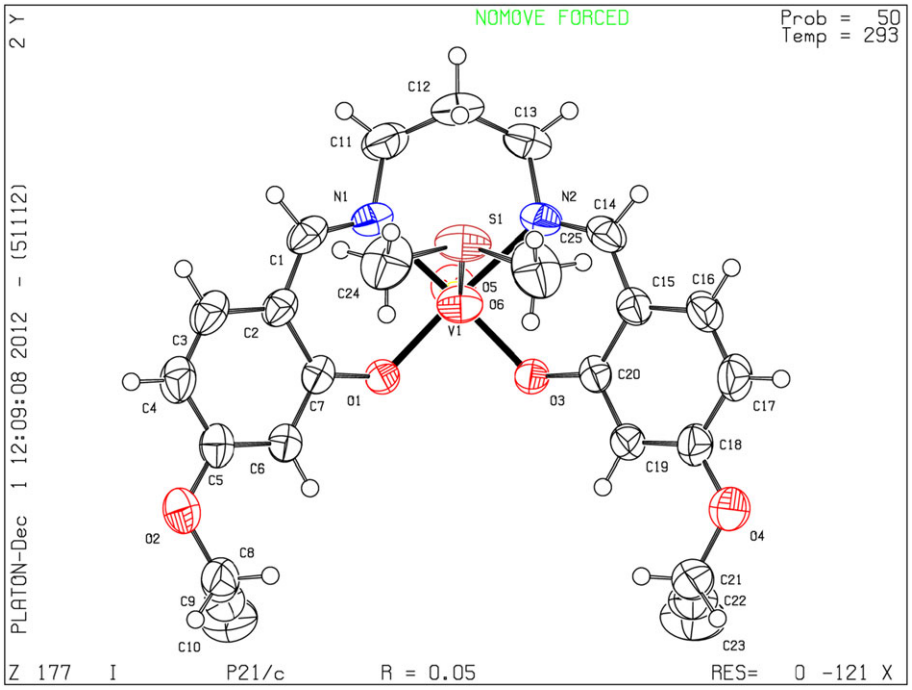

FIGURE 1 ORTEP view of VOL^2 (50% probability level)

angles around atoms C7 (360.0(3)°) and C15 (359.0(3)°) of aromatic ring in the molecule is in accordance with sp^2 hybridization. The bond lengths of N(1)-V(1), N(2)-V(1), phenoxy O(1)–V(1), and O(3)–V(1) are 2.093(3) Å, 2.098(3) Å, 1.951(2) Å and 1.963(2) Å, respectively. The bond angles O(1)–V(1)–O(3), O(1)–V(1)–N(1) and N(1)–V(1)–N(2) are 86.51(9), 88.19(10) and 92.62(11), respectively. The apical position is occupied by the oxo ligand. The terminal V–O_{oxo} bond distance of 1.605(2) Å and the vanadium displaced from mean plane of the four N2O2 is approximately 0.22 Å, which is a value characteristic of six-rather than five-coordination. The solvent dimethyl sulfoxide group shows an extended conformation values of [V1–O6–S1–C24] is +125.7(2)° and [V1–O6–S1–C25] is −130.6(2)°] positive anti-clinal and negative anti-clinal conformation. The bond length and bond angle distances well harmonize with the corresponding values reported for the related systems (Table S2).[32] In addition, the bond valence sum (BVS) calculated for the V center in VOL^1 (3.66), VOL^2 (3.74) and VOL^3 (3.68) clearly suggest an oxidation state of +4 for vanadium in these compounds (Table S3).

3.3 | FT-IR spectra

The free Schiff bases exhibit a broad band between 3450 and 3200 cm^{-1} with a maximum at 3406 and 3385 cm^{-1} is attributed to the phenolic hydroxyl ν(O–H) frequency with O–H···N intramolecular hydrogen bonding. This bond is absent in the vanadium complexes indicating that the hydroxyl oxygen atom is coordinated to vanadium with deprotonation (Figure S2). On the other hand, the phenolic oxygen ν(C-O), which occurs in the region 1301–1307 cm^{-1} for the Schiff bases, moved to higher frequencies after complexation (Table S4). The azomethine stretching frequency of the free ligands appeared in the range of 1625–1631 cm^{-1} has been shifted to lower frequencies in metal complexes suggest that azomethine nitrogen is coordinated to the vanadium ions. The high intensity sharp band observed in the region of 879–

TABLE 1 Crystallographic parameters for VOL^2 complex

Parameters	VOL^2	
Empirical formula	C_{25} $H_{26}N_2O_6$ SV	
Formula weight	533.48	
Temperature (K)	293 (2)	
Wavelength (Å)	0.71073	
Crystal system, Space group	Monoclinic, $P2_1/c$	
Unit cell dimensions	a = 16.0613(9) Å b = 7.6951(3) Å c = 22.1374(11) Å	α = 90° β = 112.226(2)° γ = 90°
Volume ($Å^3$)	2532.7(2)	
Z, D_{cal} (Mgm^{-3})	4, 1.399	
Absorption coefficient (mm^{-1})	0.516	
F(000)	1108	
Crystal size (mm)	0.25 × 0.23 × 0.20	
Theta range for data collection (°)	1.94 to 28.32	
Limiting indices	18 < =h < =21, −10 < =k < =10, −29 < =l < =27	
Reflections collected / unique	24510 / 6284	
R (int)	0.0782	
Completeness θ = 25°	99.9%	
Refinement method	Full-matrix least-squares on F^2	
Data / restraints / parameters	6284 / 0 / 316	
Goodness-of-fit on F^2	1.015	
Final R indices [$I > 2\sigma$(I)]	R1 = 0.0542, wR2 = 0.1338	
R indices (all data)	R1 = 0.1079, wR2 = 0.1600	
Largest diff. peak and hole ($e.Å^{-3}$)	0.416 and −0.479	

904 cm^{-1} is attributed to the V = O vibrations indicating the monomeric nature of the vanadium complex with no intermolecular interaction with participation of the V = O moiety in the solid state. The single crystal XRD studies also confirm this nature of binding.

3.4 | Electronic absorption spectra and magnetic moment

The absorption spectra of VOL^1-VOL^3 were recorded in acetonitrile at room temperature (Figure S3) and the band assignments are given in Table 2. The Schiff bases show two strong bands appear in the region 275–304 nm for para substituted benzene compound and third band in the region 385–387 nm for π-π* transition of azomethine group. The complexes show a strong band observed around 454–459 nm is due to the enolate oxygen to vanadium(IV) transition. The low intensity *d-d* band around 570–583 nm is due to the ligand field transition d_{xz}, d_{yz}, to d_{xy} of the VO^{2+} center. The calculated magnetic moment values of vanadium complexes are in the range of 1.73–1.78BM at room temperature are consistent with the spin only value corresponds to the paramagnetic nature of mononuclear complexes in d^1 system.[33]

In order to get more information on the nature of transitions in electronic absorption spectra of VOL^1-VOL^3, TD-DFT calculations using B3LYP/6-311G(d,p) level were carried out. All the vanadium complexes show a high energy absorption band in the range 285–403 nm can be attributed to the LMCT or MLCT charge transfer transitions. The spectra show one lowest energy absorption band in the range 542–579 nm can be attributed to the d-d transitions,[33] (Table S5). The calculated values agree well with the experimental values. The FMO diagram and calculated absorption spectra of all the vanadium complexes were given in Figures S4 and S5.

3.5 | EPR spectra

The VOL^1-VOL^3 exhibit well resolved axial anisotropy with eight line hyperfine splitting pattern in acetonitrile medium at 77 K (Figures 2 and S6). This is due to the unpaired electron of the ^{51}V nucleus ($I = 7/2$) and indicates the presence of mononuclear oxovanadium(IV) species. The spin Hamiltonian parameters and the hyperfine coupling constants calculated, $g_{\parallel} < g_{\perp}$ and $A_{\parallel} > A_{\perp}[g_{\parallel}$ (1.96–1.97) and $g_{\perp}$ 2.03] suggest that the metal complex has an axially compressed octahedral geometry around the V(IV) center with an unpaired electron in the d_{xy} orbital. The calculated G values are in the range of 4.1–6.8 demonstrates that the exchange interaction between the vanadium ions is negligible. The molecular orbital coefficients σ bonding (α^2) and π bonding (β^2) were

TABLE 2 Electronic absorption spectral data of vanadium complexes in acetonitrile

Complex	λ_{max} (nm)	Assignments	Geometry	μ_{eff} (BM)
VOL^1	459 575	$^2B_2 \rightarrow {}^2B_1$ $^2B_2 \rightarrow {}^2E$	Distorted octahedral	1.73
VOL^2	454 570	$^2B_2 \rightarrow {}^2B_1$ $^2B_2 \rightarrow {}^2E$	Distorted octahedral	1.78
VOL^3	416 583	$^2B_2 \rightarrow {}^2B_1$ $^2B_2 \rightarrow {}^2E$	Distorted octahedral	1.73

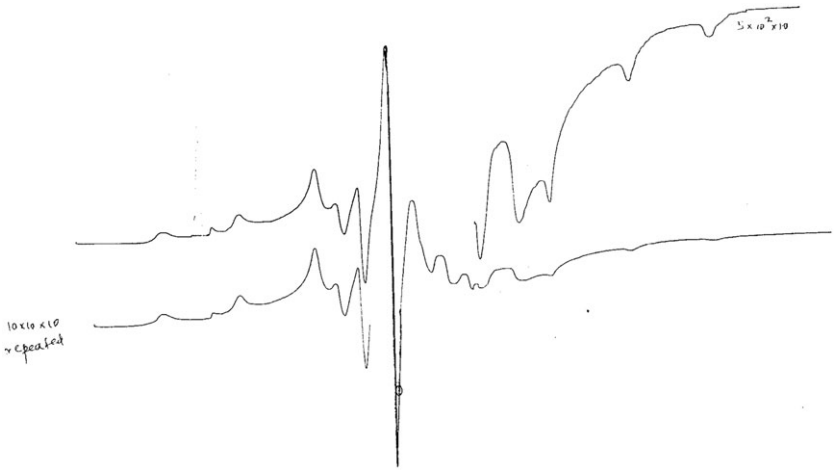

FIGURE 2 EPR spectrum of VOL^1 at 77 K in acetonitrile

calculated. The calculated values suggest that in-plane bonding (σ) is more covalent than out of plane bonding (π) (Table 3).

3.6 | Electrochemistry

The electrochemical property of VOL^1-VOL^3 in acetonitrile was studied by recording the cyclic voltammograms. All the three complexes exhibit similar voltammograms in the negative region (0.0 to −1.0 V) containing an oxidation and corresponding reduction process with one electron transfer (Figure S7). The VOL^1-VOL^3 shows a quasi-reversible single electron wave at the potential range of ~ − 0.621 V, which is assigned to the reduction of V(IV) to V(III). The corresponding oxidation process occurs in the potential of ~ − 0.48 V.[34]

TABLE 3 Spin Hamiltonian parameters of vanadium complexes in acetonitrile

Complex	A_{II} ×10^{-4}	$A_\perp$	A_{av}	g_{II}	$g_\perp$	g_{av}	G	$\frac{g_{II}}{A_{II}}$	K_{II}	$K_\perp$	α^2	β^2	γ^2
VOL^1	165	77	106	1.92	2.02	1.98	4.6	116	0.31	0.38	0.53	0.58	0.72
VOL^2	161	81	108	1.93	2.02	1.99	4.1	120	0.40	0.47	0.61	0.65	0.75
VOL^3	178	79	112	1.95	2.01	1.99	6.8	109	0.44	0.47	0.64	0.68	0.73

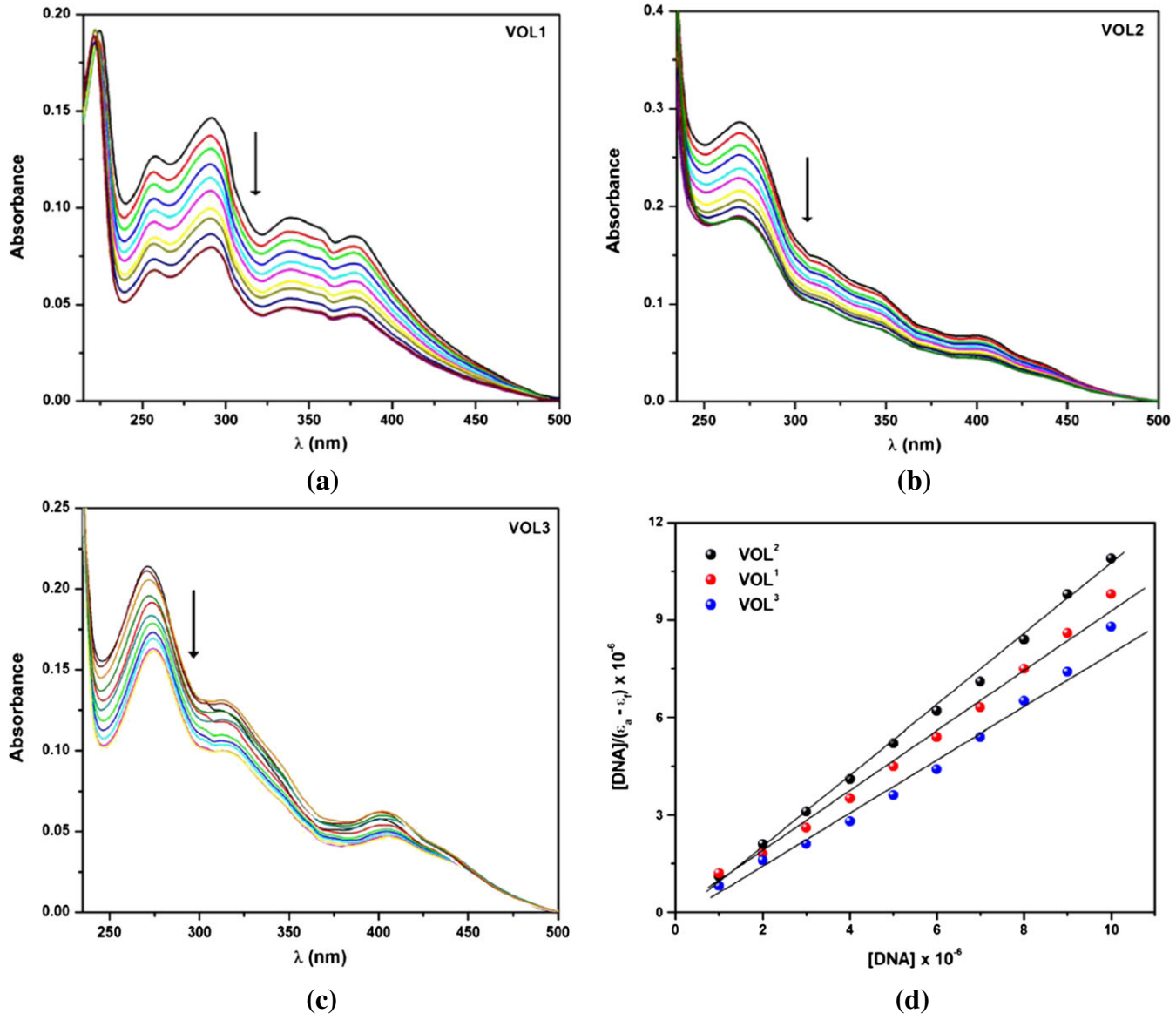

FIGURE 3 Absorption spectra of **(a)** VOL^1; **(b)** VOL^2 and **(c)** VOL^3 (40 μM) with increasing amount of CT-DNA; **(d)** plot of $[DNA]/(\varepsilon_a - \varepsilon_f)$ vs [DNA] for VOL^1-VOL^3 with CT-DNA

3.7 | DNA binding study

3.7.1 | Absorption spectral study

Electronic absorption spectral titration method was employed to find out the binding interaction of VOL^1-VOL^3 with DNA. Metal complexes bind to DNA by intercalation are distinguished by the change in absorbance and bathochromic shift in wavelength. The electronic absorption study was carried out by maintaining the concentration of vanadium complex constant (40 μM) and varying the concentration of CT-DNA (0.0-100 μM). Upon the incremental addition of CT-DNA with VOL^1-VOL^3, the absorption intensity was gradually decreased (hypochromism) in the region of 260–305 nm by 25%, 22% and 16% respectively along with a bathochromic shift of 2–5 nm (Figure 3). This may be due to the interaction between aromatic chromophore in the vanadium complex and base pairs of DNA.[35] The observed results suggest that all the VOL^1-VOL^3 were bound to CT-DNA through intercalative mode[36] and follows the order $VOL^1 < VOL^3 < VOL^2$. In general, the flat-electron rich aromatic compounds strongly interact with DNA base pairs. The complex, VOL^1 and VOL^3 are formed with

TABLE 4 DNA association constant (K_b), Stern-Volmer constant (K_q) and apparent binding constant (K_{app}) for VOL^1-VOL^3

Complexes	K_b $(M^{-1})\times 10^5$	K_q $(M^{-1}) \times 10^5$	n	K_{app} $(M^{-1}) \times 10^6$
VOL^1	3.66	2.24	3.4	4.96
VOL^2	5.19	3.21	4.9	4.42
VOL^3	4.01	2.58	4.1	4.71

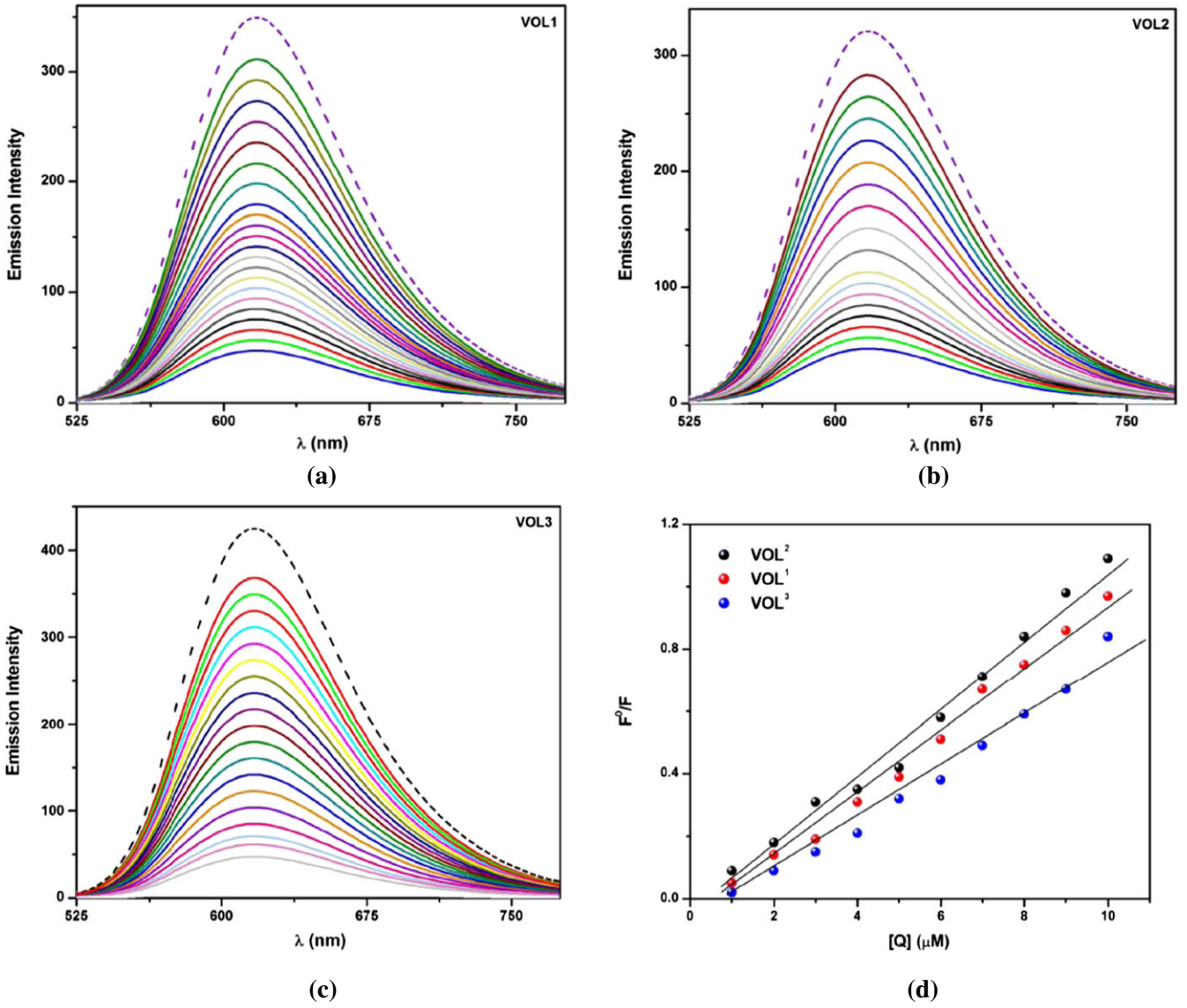

FIGURE 4 Emission quenching curves of EB bound to CT-DNA in the presence of, **(a)** VOL^1; **(b)** VOL^2 and **(c)** VOL^3 (0.0–100 μM) in Tris–HCl buffer. (d) Stern-Volmer plot of VOL^1-VOL^3 with CT-DNA

five-membered chelate rings, but the complex VOL^2 has six-membered chelate rings. The complex VOL^2 with six-membered chelate rings easily and strongly interact with DNA base pairs and has higher DNA binding affinity value than the VOL^1 and VOL^3. The presence of methyl group in L^1 may be the reason for the difference in binding ability of VOL^1 and VOL^3 with DNA. The intrinsic binding constants (K_b) values are listed in Table 4 and are compared with similar type of compounds (Table S6). From the results, it is clear that the complexes interact with DNA through intercalation and show similar binding affinity towards DNA.

3.7.2 | Fluorescence quenching study

The binding affinity of VOL^1-VOL^3 with DNA was further examined using fluorescence quenching experiments, based on the dislocation of ethidium bromide (EB) from CT-DNA base pairs. The groove binders and intercalators can decrease the fluorescence intensity of EB-DNA adduct by replacing the EB and/or by tolerant the excited state electron of EB via photo-electron transfer mechanism.[37] The EB molecule has very weak emission intensity in Tris-HCl buffer. But the emission intensity of EB is significantly increased due to the intercalation into the double helical structure of DNA base pairs. After the additions of VOL^1-VOL^3 to EB-DNA, the emission intensity of EB-DNA adduct was significantly decreased of ca. 36%, 43% and 40%, respectively. The observed results suggest that all the vanadium complexes competitively bind to DNA (Figure 4). The calculated quenching constant values and number of binding sites ($K_q = 3.21 \times 10^5$; $n = 4.9$) suggest that the quenching efficiency of VOL^2 complex is higher than the VOL^1 ($K_q = 2.24 \times 10^5$; $n = 3.4$) and VOL^3 ($K_q = 2.58 \times 10^5$; $n = 4.1$) complexes, which is agreement with the electronic absorption titrations data. In addition, the apprent binding constant (K_{app}) value of complexes were calculated using the equation, $K_{EB}[EB] = K_{app}[compound]$, where [EB], $K_{EB} = 1.0 \times 10^7\ M^{-1}$ is the complex concentration has the value at 50% reduction ofthe emission intensity and [EB] = 2.5 μM (Table 4). The quenching and binding constant values indicate that all the VOL^1-VOL^3 interact with CT-DNA via intercalation mode.[38]

3.7.3 | DNA melting study

DNA helix melting studies were carried out to predict the binding character of complexes to DNA and their relative binding strength.[39] The melting temperature represents the breaking of hydrogen bonds between the double stranded DNA base pairs to form the single stranded DNA. The high melting temperature (ΔT_m) value is suggestive of an intercalative binding mode between the metal complex and DNA, whereas the low melting temperature value (1–3 °C) point out a non-intercalative binding mode.[40] The helix melting curves of DNA (200 μM) in the absence and presence of complexes (VOL^1-VOL^3) (20 μM) are depicted in Figure 5a. The observed ΔT_m values demonstrate that all the vanadium complexes bind to DNA via intercalation mode.

3.7.4 | Viscosity studies

To understand the binding interaction between the vanadium complex and DNA, viscosity studies were done on CT-DNA by the addition of different concentration of VOL^1-VOL^3. Generally, optical and photophysical studies givethe clues about the binding, that are essential, but not enough to predict the binding mode between DNA

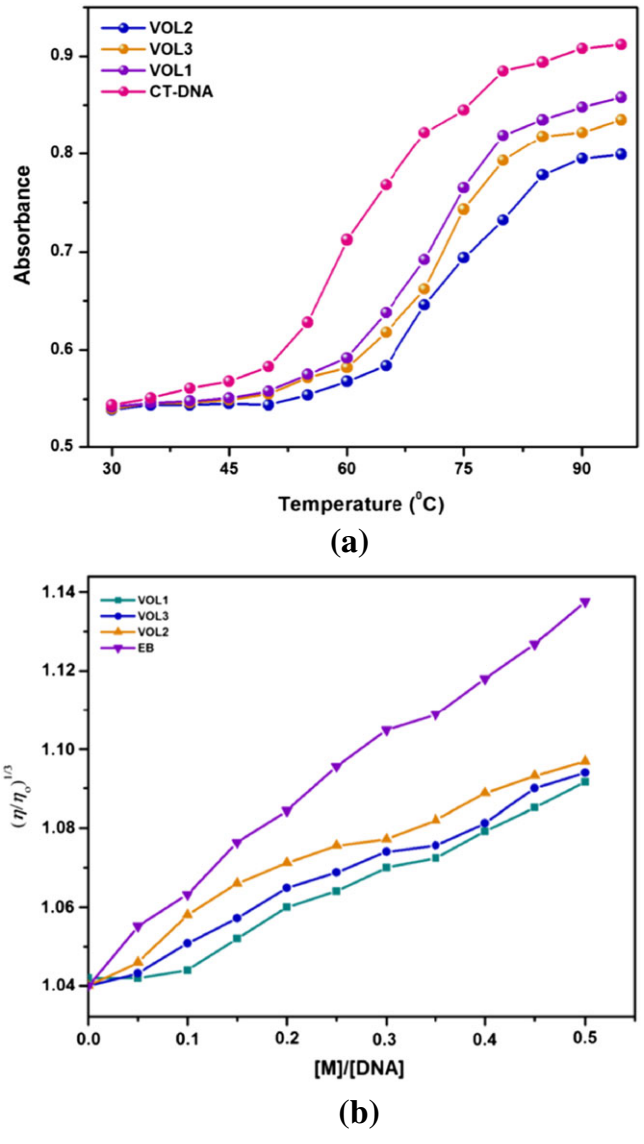

FIGURE 5 (a) Thermal melting profiles of CT-DNA with VOL^1-VOL^3 and (b) effects of increasing concentrations of VOL^1-VOL^3 on the relative viscosities of CT-DNA

and metal complexes. The viscosity measurements are used to predict the binding model in solution. When a metal complex interacts with DNA through classical intercalation binding mode results lengthening of DNA helix and break the hydrogen bond between the base pairs, which leads to an increase in DNA viscosity. The partial and/or non-classical intercalation of complex results bend or kink the DNA helix leads to decrease of the viscosity of DNA.[41] Upon the incrimental addtition of VOL^1-VOL^3, the relative viscosity of CT-DNA was significantly increased and the obtained results suggest that the complexes are inserted between the DNA bases

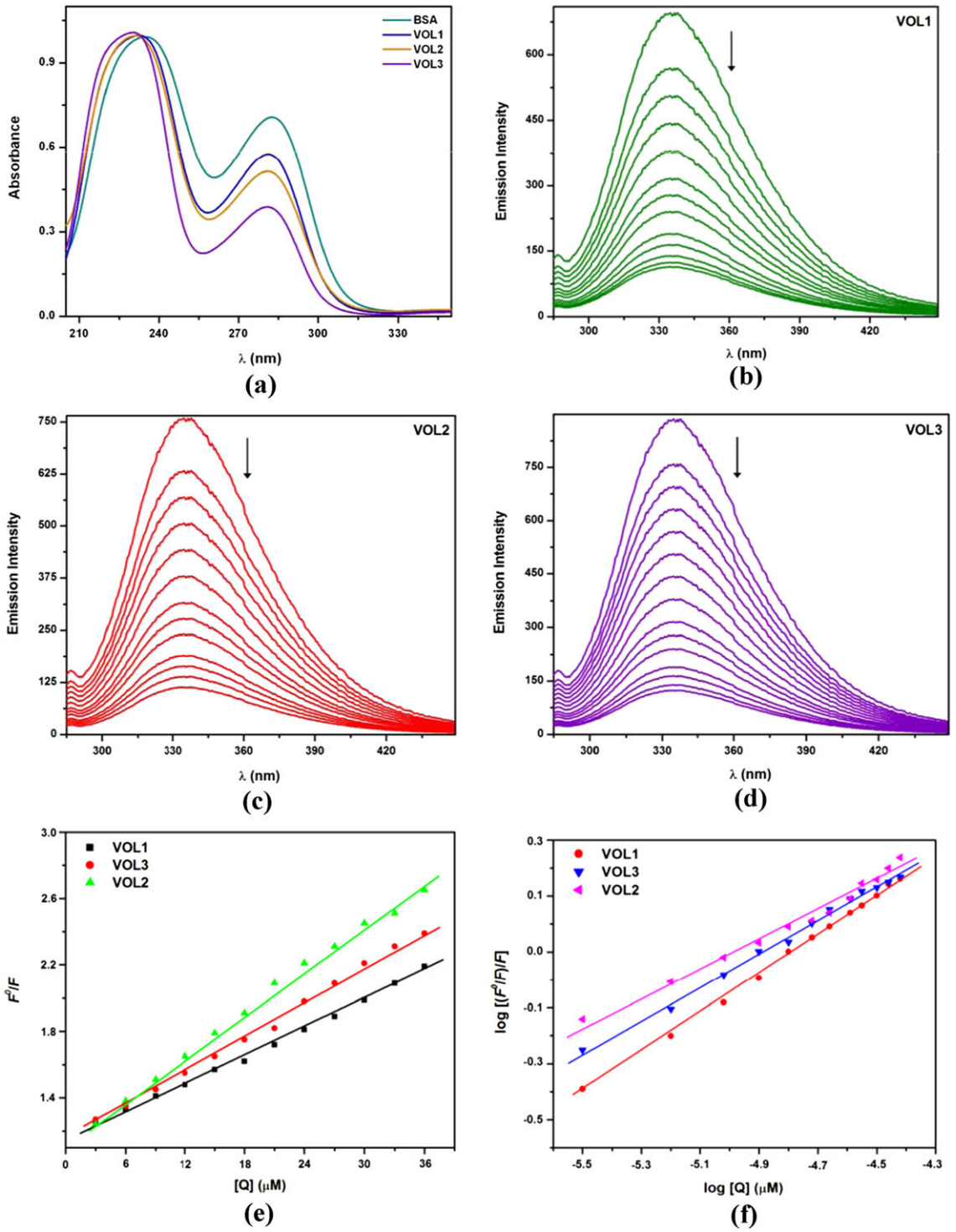

FIGURE 6 **(a)** Electronic absorption spectra of BSA protein with VOL^1-VOL^3; **(b-d)** emission quenching spectra of BSA in the presence of increasing amounts of **(b)** VOL^1; **(c)** VOL^2 and **(d)** VOL^3. [BSA] = 1 μM and [complex] = 0–50 μM; **(e)** stern-Volmer plot for VOL^1-VOL^3 with BSA protein; **(f)** Scatchard plot for VOL^1-VOL^3 with BSA protein

(Figure 5b) through intercalation and the binding between the vanadium complex and CT-DNA follows the order $VOL^1 < VOL^3 < VOL^2$.

3.8 | Protein binding studies

The absorption spectra of protein (BSA) with VOL^1-VOL^3 were carried out to predict the type of quenching process. Addition of vanadium complexes to BSA protein, the absorption band at 281 nm is increased without any shift (Figure 6a). The observed results suggest that the binding of vanadium complexes with BSA protein through static quenching process.[36] The structural changes of BSA protein upon the addition of vanadium complexes were studied by fluorescence spectral method (excitation at 281 nm) in the wavelength range of 290–450 nm. A 1.0×10^{-6} M solution of protein was titrated with different concentrations of vanadium complexes (0.0–50 μM). Upon the addition of vanadium complex, the emission intensity at 340 nm is gradually decreased due to the interaction of the complex hydrophobically with the BSA protein (Figure 6b-d).[42] The fluorescence quenching was explained by Stern-Volmer relation,

$$F_0/F = 1 + K_{sv}[Q]$$

Where F_0 and F are the emission intensities of absence and presence of vanadium complexes. K_{sv} is linear Stern-Volmer quenching constant and $[Q]$ is the concentration of complexes. The K_{sv} can be calculated using the plot of (F_0/F) versus log $[Q]$ (Figure 6e). The small molecules bind in parallel to a set of equivalent site on a macromolecule and the equilibrium between free and bound molecules is established by Scatchard equation,[43]

$$\log[(F_0 - F)/I] = \log K_b + n \log[Q]$$

where K_b is the binding constant of vanadium complexes with protein and n is the number of binding sites. The binding constant (K_b) values and the number of binding sites (n) were calculated from the plot of $\log[(F_0 - F)/F]$ versus $\log[Q]$ (Figure 6f). The observed results clearly indicate that the vanadium complexes have only one binding site is existing to interact with protein molecules (Table 5).

TABLE 5 BSA protein binding constant (K_b), quenching constant (K_q) and number of binding sites (n) for VOL^1-VOL^3

Complex	K_b (M^{-1}) × 10^6	K_{sv} (M^{-1}) × 10^5	n
VOL^1	3.95	3.54	1.08
VOL^2	4.22	3.78	1.02
VOL^3	4.03	3.66	0.98

3.9 | Synchronous emission spectra

To get information about the molecular microenvironment of the protein, synchronous emission spectra of protein in the absence and presence of vanadium complexes were studied. The protein containing amino acids (tyrosine, tryptophan and phenylalanine) is responsible for the fluorescence property of BSA protein. The excitation and emission wavelengths ($\Delta\lambda = \lambda_{em} - \lambda_{ex}$) reflect the nature of the chromophore.[44,45] The small $\Delta\lambda$ value (15 nm) is due to the tyrosine residue, whereas a large $\Delta\lambda$ value (60 nm) is characteristic of tryptophan residue.[46] Upon the addition of vanadium complexes, the emission intensity of tryptophan and tyrosine residue was decreased at 302 nm and 342 nm, respectively (Figures S8 and S9). The observed results indicate that the interaction of vanadium complexes with BSA protein provoked micro-environmental and conformational changes in the BSA protein.[47]

3.10 | Chemical nuclease activity

DNA cleavage ability of VOL^1-VOL^3 was evaluated with pUC19DNA. In general, metal complexes cleave pUC19DNA with or without any external agents, and as a result supercoiled form (Form I) of DNA relaxed to open circular nicked form (Form II). Usually, Form I migrates faster than the Form II on electrophoresis and further cleaved to generate a linear form (Form III), which migrates between the Form I and Form II.[48] In the absence of vanadium complexes, no distinct cleavage pattern was observed in the DNA (lane 1). In the absence of external agents such as H_2O_2, the vanadium complexes were not able to cleave the DNA (Lane: 2–4). But in the presence of H_2O_2, all the complexes cleave the DNA and transform the supercoiled form of DNA (Form I) into open circular

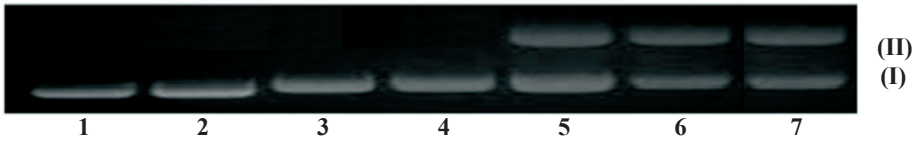

FIGURE 7 DNA cleavage activity of VOL^1-VOL^3, lane 1: Control; lane 2: DNA + VOL^1; lane 3: DNA + VOL^2; lane 4: DNA + VOL^3; lane 5; DNA + VOL^1 + H_2O_2; lane 6: DNA + VOL^2 + H_2O_2; lane 7: DNA + VOL^3+ H_2O_2

nicked form (Form II, Lane: 5–7) (Figure 7). The observed results suggest that all the vanadium complexes can efficiently cleave the plasmid DNA in the presence of H_2O_2. This suggests that the DNA cleavage intervened by vanadium complexes should adopt an oxidative mechanism.

In oxidative DNA cleavage, the transition-metal-mediated hydroxyl radical production occurs through two well-known pathways such as Fenton and Haber-Weiss mechanism. The Haber-Weiss reaction is the most feasible mechanism for the DNA cleavage induced by the metal complexes. Haber-Weiss reaction involves the reaction of superoxide with H_2O_2 to produce O_2, hydroxide and $OH^{\bullet}$. The probable mechanism of DNA damage induced by metal complexes is follows,

$$VO^{2+} + e^{-} \rightarrow VO_2^{+}$$

$$VO^{2+} + O_2 \rightarrow VO^{2+} + O_2^{-}\bullet$$

$$O_2^{-}\bullet + H_2O_2 \rightarrow O_2 + OH^{\bullet} + OH^{-}$$

The generation of $OH^{\bullet}$ radical, superoxide anion and hydrogen peroxide are responsible for the cleavage of DNA by complexes. The abstraction of H atom by the reactive $OH^{\bullet}$ radical from deoxyribose sugar may be the reason for the cleavage of pUC19 DNA. The results suggest that the oxidative process is involved in the DNA cleavage reaction.[49]

3.11 | Antioxidant property

DPPH assay has been widely used to investigate the scavenging activities of several compounds. DPPH radical was scavenged by antioxidants through the donation of hydrogen or electron, forming the reduced DPPH-$H^{\bullet}$. The stable DPPH radical has absorption maximum centered at about 517 nm. When an electron or a free radical species is absorbed results in discoloration from purple to yellow and the absorption band disappears. Addition of the compounds reduces the intensity of absorption of DPPH radical. The radical-scavenging activity of the Schiff bases (L^1-L^3) and their vanadium complexes (VOL^1-VOL^3) in methanol are given in Figure S10. The 50% inhibitory concentration (IC_{50}) values imply that the scavenging effect of the compounds follows the order VOL^1-VOL^3 > L^2 > L^3 > L^1 (Table S7). The IC_{50} values of vanadium complexes are close to the value of the control, ascorbic acid (11.55 μM). The results obtained clearly indicate that the vanadium complexes are good antioxidants.

3.12 | Antibacterial activity

The Schiff bases and their vanadium(IV) complexes (VOL^1-VOL^3) were screened for their *in vitro* antimicrobial activities against gram positive *Staphylococcus aureus* and *Bacillus subtilis* bacteria and gram negative *Pseudomonas aeruginosa* and *Escherichia coli* bacteria to assess their potential antimicrobial activity. The zone of inhibition of the vanadium complexes were compared with the Schiff bases (L^1-L^3) and the control, ampicillin (Figure S11). Comparative antibacterial studies show that the inhibition order follows: Ampicillin > vanadium complex > Schiff bases (Table S8). The antibacterial activity increases with increasing the concentrations of the compounds, but they are still lower than that of the control. The antibacterial activity of vanadium complexes may be due to the contact antibacterial mechanism or the stripping antibacterial mechanism or the both. In the contact antibacterial mechanism, the vanadium metal quickly attaches with the –SH of pheron in the bacterial body terminates the metabolism process due to the loss of action of enzyme of the organism and killed the bacteria. In the stripping antibacterial mechanism, the antibacterial ions stripping from the antibacterial material react with the protein deactivates the enzymes of the organism, which results in termination of metabolism process and death of the bacteria.

3.13 | Bio-mimicking catalytic Bromination reaction (phenol red to bromophenol blue)

Vanadium dependent haloperoxidase catalyzes many organic compounds by oxidative halogenation in the presence of halide ions and hydrogen peroxide. Several oxovanadium complexes catalyze the bromination of organic substrates in the presence of bromide ions and H_2O_2 and mimic the vanadium haloperoxidases. The bromoperoxidase activity of the enzymes and their model complexes is determined by the kinetic study of the oxidative bromination of phenol red to bromophenol blue.[50] The catalytic activity of VOL^1-VOL^3 was evaluated using phenol red as model substrate and the reaction was monitored by UV–Vis spectrophotometric method (Scheme S1). The absorption band of phenol red was gradually decreased at 441 nm with VOL^1, 439 nm with VOL^2 and 440 nm with VOL^3 and a new peak appeared at 586 nm (VOL^1), 588 nm (VOL^2) and 591 nm (VOL^3) is due to formation of bromophenol as product (Figure 8a-c). The isosbestic points at 494 nm (VOL^1), 494 nm (VOL^2) and 495 nm (VOL^3) shows the conversion of phenol red to bromophenol blue and the reaction was completed after ~2 h under ambient conditions. The kinetic

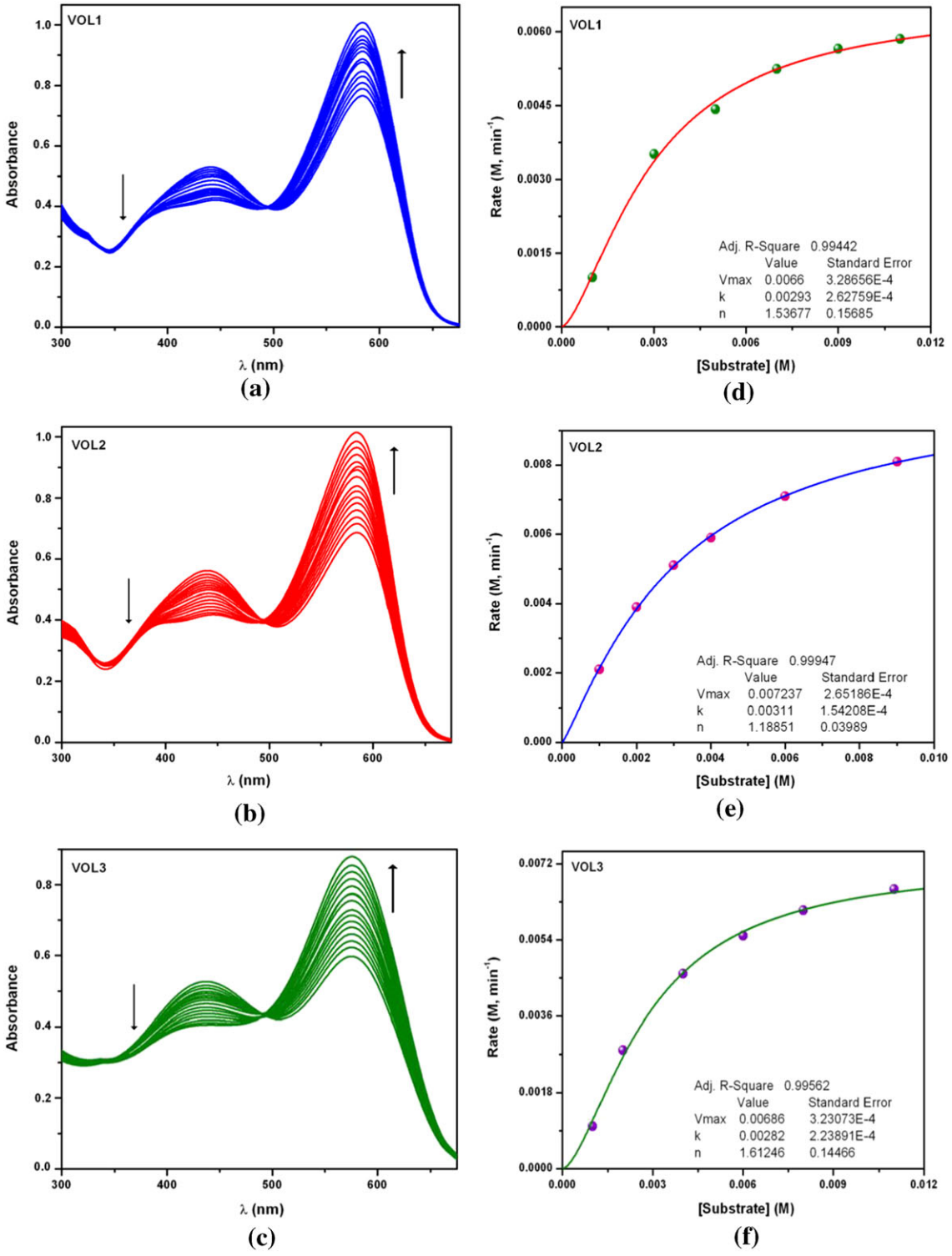

FIGURE 8 (**a-c**) Oxidative bromination of phenol red catalyzed by VOL^1-VOL^3 in aqueous phosphate buffer at pH = 7.2; (**d-f**) initial rates versus substrate concentrations for bromination reaction catalyzed by VOL^1-VOL^3

studies of the plots for the above conversion are given in Figure 8d-f and the reaction exhibits saturation kinetics based on the Michaelis–Menten model. Michaelis binding constant (K_m), maximum velocity (V_{max}) and rate constant for dissociation of substrates (k_{cat}) were calculated from the Lineweaver-Burk graph of 1/rate versus 1/[S] (Figure S12), using the equation $1/V = (K_M/V_{max})(1/[S]) + 1/V_{max}$ (Table 6). A control reaction was carried out without the vanadium complex shows no appreciable change in the absorbance (Figure S13).

TABLE 6 Kinetic parameters for bromination of phenol red by VOL^1-VOL^3

Complex	V_{max} (M min^{-1})	K_M (M)	k_{cat} (h^{-1})
VOL^1	6.60×10^{-3}	2.93×10^{-3}	396.0
VOL^2	7.24×10^{-3}	3.11×10^{-3}	434.2
VOL^3	6.86×10^{-3}	2.82×10^{-3}	411.6

4 | CONCLUSION

Three vanadium(IV) Schiff base complexes (VOL^1-VOL^3) containing -O and -N ligation sites were synthesized and characterized by various spectral techniques. Distorted octahedral geometry for VOL^2 is confirmed by the single crystal XRD studies reveal that the V(IV) center of the complex is hexacoordinated in a VO4N2 coordination with basal plane by the Schiff base molecule. The complexes exhibit quasi-reversible single electron wave at the potential range of ~ −0.621 V − 0.48 V. The DNA binding studies suggest that the complexes interact with DNA through intercalation. The protein binding studies reveals that the complexes quench the intrinsic fluorescence of BSA via static quenching mechanism. The chemical nuclease activity studied indicates that the complexes cleave the DNA in the presence of H_2O_2. The DPPH studies show higher scavenging activity of the complexes than the Schiff bases. The complexes exhibit better antibacterial activity. To develop model metal complexes mimicking vanadium dependent haloperoxidase, the biocatalytic activity of the synthesized complexes were evaluated. The vanadium complexes exhibit enzyme mimetic catalytic activities as a bromoperoxidase and as a chemical nuclease.

Supplementary Materials

The experimental part on binding interactions and catecholase activity are given in the supplementary. CCDC 882669 contains the supplementary crystallographic data for VOL^2. These data can be obtained free of charge viahttp://www.ccdc.cam.ac.uk/conts/retrieving.html, or from the Cambridge Crystallographic Data Centre, 12 Union Road, Cambridge CB2 1EZ, UK; fax: (+44) 1223–336-033; or email: deposit@ccdc.cam.ac.uk.

ACKNOWLEDGEMENT

Financial supports received from the Science and Engineering Research Board (SERB), Department of Science and Technology (DST), Government of India, New Delhi (EMR-II/2014/000081) is gratefully acknowledged. SAIF-STIC, Cochin is acknowledged for CHNS and single crystal XRD analysis.

ORCID

M.A. Neelakantan http://orcid.org/0000-0002-6321-0668

REFERENCES

[1] a) K. D. Karlin, *Progress in Inorganic Chemistry*, John Wiley & Sons, Inc., Hoboken, NJ **2012**. b) A. Ali, M. Kamra, A. Bhan, S. S. Mandal, S. Bhattacharya, *Dalton Trans.* **2016**, *45*, 9345.

[2] N. Hadjiliadis, E. Sletten, *Metal Complex – DNA Interactions*, John Wiley & Sons Ltd., The Atrium, Southern Gate, Chichester **2009**.

[3] a) V. Selvarani, B. Annaraj, M. A. Neelakantan, S. Sundaramoorthy, D. Velmurugan, *Polyhedron* **2013**, *54*, 74. b) B. Annaraj, C. Balakrishnan, M. A. Neelakantan, *J. Photochem. Photobiol. B* **2016**, *160*, 278.

[4] G. Zuber, J. C. Quada, S. M. Hecht, *J. Am. Chem. Soc.* **1998**, *120*, 9368.

[5] S. Feng, R. Xu, *Acc. Chem. Res.* **2001**, *34*, 239.

[6] D. Rehder, *Dalton Trans.* **2013**, *42*, 11749.

[7] E. C. Theil, K. N. Raymond, I. Bertini, H. B. Gray, S. J. Lippard, J. S. Valentine, University Science Books, Mill Valley, CA, **1994**, 1.

[8] D. C. Crans, J. J. Smee, E. Gaidamauskas, L. Yang, *Chem. Rev.* **2004**, *104*, 849.

[9] A. Butler, J. V. Walker, *Chem. Rev.* **1993**, *93*, 1937.

[10] R. Wever, B. E Krenn, N. D. Chasteen, Ed., Kluwer Academic Publishers, Dordrecht, **1990**, 81.

[11] M. G. Almeida, M. Humanes, R. Melo, J. A. Silva, J. J. R. F. da Silva, R. Wever, *Phytochemistry* **2000**, *54*, 5.

[12] G. J. Colpas, B. J. Hamstra, J. W. Kampf, V. L. Pecoraro, *J. Am. Chem. Soc.* **1996**, *118*, 3469.

[13] J. N. C. Franklin, A. Butler, *J. Am. Chem. Soc.* **2004**, *126*, 15060.

[14] a) M. N. Islam, A. A. Kumbhar, A. S. Kumbhar, M. Zeller, R. J. Butcher, M. B. Dusane, B. N. Joshi, *Inorg. Chem.* **2010**, *49*, 8237. b) A. M. Evangelou, *Crc. Cr. Rev. Oncol-Hem.* **2002**, *42*, 249.

[15] J. Y. Kravitz, V. L. Pecoraro, *Pure Appl. Chem.* **2005**, *77*, 1595.

[16] a) M. R. Maurya, B. Uprety, F. Avecilla, P. Adao, J. C. Pessoa, *Dalton Trans.* **2015**, *44*, 17736. b) S. P. Dash, A. K. Panda, S. Dhaka, S. Pasayat, A. Biswas, M. R. Maurya, P. K. Majhi, A. Crochet, R. Dinda, *Dalton Trans.* **2016**, *45*, 18292.

[17] a) S. Thalamuthu, B. Annaraj, M. A. Neelakantan, *Spectrochim. Acta, Part A* **2014**, *118*, 120. b) P. J. K. Inba, B. Annaraj, S. Thalamuthu, M. A. Neelakantan, *Spectrochim. Acta, Part A* **2013**, *104*, 300. c) C. Balakrishnan, S. Natarajan, M. A. Neelakantan, *RSC Adv.* **2016**, *6*, 102482.

[18] E. R. Milaeva, S. I. Filimonova, N. N. Meleshonkova, L. G. Dubova, E. F. Shevtsova, S. O. Bachuria, N. S. Zefirov, *Bioinorg. Chem. Appl.* **2010**, *2010*, 1.

[19] A. A. Holder, P. Taylor, A. R. Magnusen, E. T. Moffett, K. Meyer, Y. Hong, S. E. Ramsdale, M. Gordon, J. Stubbs, L. A. Seymour, D. Acharya, R. T. Weber, P. F. Smith, G. C. Dismukes, P. Ji, L. Menocal, F. Bai, J. L. Williams, D. M. Cropek, W. L. Jarrett, *Dalton Trans.* **2013**, *42*, 11881.

[20] L. X. Cheng, J. J. Tang, H. Luo, X. L. Jin, F. Dai, J. Yang, Y. P. Qian, X. Z. Li, B. Zhou, *Bioorg. Med. Chem. Lett.* **2010**, *20*, 2417.

[21] W. Maruyama, M. Naoi, *Mech. AgeingDev.* **1999**, *111*, 189.

[22] Bruker, APEX2, SAINT and SADABS. Bruker AXS Inc. Madison, WI, **2008**.

[23] G. M. Sheldrick, SHELXS-97 and SHELXL-97, Program for the Solution of Crystal Structures, University of Gottingen, Gottingen, **1997**.

[24] M. J. Frisch, G. W. Trucks, H. B. Schlegel, G. E. Scuseria, M. A. Robb, R. J. Cheeseman Jr., J. A. Montgomery, T. Vreven, K. N. Kudin, J. C. Burant, J. M. Millam, S. S. Iyengar, J. Tomasi, V. Barone, B. Mennucci, M. Cossi, G. Scalmani, N. Rega, G. A. Petersson, H. Nakatsuji, M. Hada, M. Ehara, K. Toyota, R. Fukuda, J. Hasegawa, M. Ishida, T. Nakajima, Y. Honda, O. Kitao, H. Nakai, M. Klene, X. Li, J. E. Knox, H. P. Hratchian, J. B. Cross, C. Adamo, J. Jaramillo, R. Gomperts, R. E. Stratmann, O. Yazyev, A. J. Austin, R. Cammi, C. Pomelli, J. W. Ochterski, P. Y. Ayala, K. Morokuma, G. A. Voth, P. Salvador, J. J. Dannenberg, V. G. Zakrzewski, S. Dapprich, A. D. Daniels, M. C. Strain, O. Farkas, D. K. Malick, A. D. Rabuck, K. Raghavachari, J. B. Foresman, J. V. Ortiz, Q. Cui, A. G. Baboul, S. Clifford, J. Cioslowski, B. B. Stefanov, G. Liu, A. Liashenko, P. Piskorz, I. Komaromi, R. L. Martin, D. J. Fox, T. Keith, M. A. A. Laham, C. Y. Peng, A. Nanayakkara, M. Challacombe, P. M. W. Gill, B. Johnson, W. Chen, M. W. Wong, C. Gonzalez, J. A. Pople, *Gaussian 03, Revision E.01*, Gaussian, Inc, Wallingford, CT **2004**.

[25] a) A. D. Becke, *Phys. Rev. A: At., Mol., Opt. Phys.* **1988**, *38*, 3098. b) C. Lee, W. Yang, R. G. Parr, *Phys. Rev. B: Condens. Matter* **1988**, *37*, 785.

[26] a) R. E. Stratmann, E. G. Scuseria, M. J. Frisch, *J. Chem. Phys.* **1998**, *109*, 8218. b) M. E. Casida, C. Jamorski, K. C. Casida, D. R. Salahub, *J. Chem. Phys.* **1998**, *108*, 4439.

[27] C. R. Merril, D. Goldman, S. A. Sedman, M. H. Ebert, *Science* **1981**, *211*, 1437.

[28] M. E. Reichmann, S. A. Rice, C. A. Thomas, P. Doty, *J. Am. Chem. Soc.* **1954**, *76*, 3047.

[29] F. Darabi, H. Hadadzadeh, M. Ebrahimi, T. Khayamian, H. A. Rudbari, *Inorg. Chim. Acta* **2014**, *409*, 379.

[30] M. Jiang, X. M. Xie, D. Zheng, Y. Liu, Y. X. Li, X. J. Chen, *J. Mol. Struct.* **2004**, *692*, 71.

[31] V. Lorian, *Antibiotics in Laboratory Medicine*, 2nd ed., Williams and Wilkins, Baltimore, MA **1986**.

[32] X. Wang, X. M. Zhang, H. X. Liu, *Polyhedron* **1995**, *14*, 293.

[33] a) M. Tsuchimoto, G. Hoshina, N. Yoshioka, H. Inoue, K. Nakajima, M. Kamishima, M. Kojima, S. Ohba, *J. Solid State Chem.* **2000**, *153*, 9. b) S. P. Dash, S. Majumder, A. Banerjee, M. F. N. N. Carvalho, P. Adao, J. C. Pessoa, K. Brzezinski, E. Garribba, H. Reuter, R. Dinda, *Inorg. Chem.* **2016**, *55*, 1165.

[34] D. Mandal, M. Chaudhury, *Struct. Chem.* **2007**, *18*, 187.

[35] D. S. Raja, N. S. P. Bhuvanesh, K. Natarajan, *Inorg. Chem.* **2011**, *50*, 12852.

[36] X. L. Wang, H. Chao, H. Li, X. L. Hong, Y. J. Liu, L. F. Tan, L. N. Ji, *J. Inorg. Biochem.* **2004**, *98*, 1143.

[37] J. K. Barton, J. M. Goldberg, C. V. Kumar, N. J. Turro, *J. Am. Chem. Soc.* **1986**, *108*, 2081.

[38] B. D. Wang, Z. Y. Yang, Q. Wang, T. K. Cai, P. Crewdson, *Bioorg. Med. Chem.* **2006**, *14*, 1880.

[39] a) S. D. Choi, M. S. Kim, S. K. Kim, P. Lincoln, E. Tuite, B. Norden, *Biochemistry* **1997**, *36*, 214. b) M. Usman, M. Zaki, R. A. Khan, A. Alsalme, M. Ahmad, S. Tabassum, *RSC Adv.* **2017**, *7*, 36056.

[40] M. Cory, D. D. Mckee, J. Kagan, D. W. Henry, J. A. Miller, *J. Am. Chem. Soc.* **1985**, *107*, 2528.

[41] S. Satyanarayana, J. C. Dabrowiak, J. B. Chaires, *Biochemistry* **1993**, *32*, 2573.

[42] D. S. Raja, N. S. P. Bhuvanesh, K. Natarajan, *Eur. J. Med. Chem.* **2011**, *46*, 4584.

[43] a) J. R. Lakowicz, Fluorescence Quenching: Theory and Applications, in *Principles of Fluorescence Spectroscopy*, Vol. 53, Kluwer Academic/Plenum Publishers, New York **1999**. b) X. Z. Feng, Z. Zhang, L. J. Yang, C. Wang, C. L. Bai, *Talanta* **1998**, *47*, 1223.

[44] G. Z. Chen, X. Z. Huang, Z. Z. Zheng, J. G. Xu, Z. B. Wang, *Analysis Method of Fluorescence*, 3rd ed., Science Press, Beijing **1990**.

[45] J. N. Miller, *Proc. Anal. Div. Chem. Soc.* **1979**, *16*, 203.

[46] a) J. H. Tang, F. Luan, X. G. Chen, *Bioorg. Med. Chem.* **2006**, *14*, 3210. b) B. Annaraj, M. A. Neelakantan, *Eur. J. Med. Chem.* **2015**, *102*, 1.

[47] P. Krishnamoorthy, P. Sathyadevi, A. H. Cowley, R. R. Butorac, N. Dharmaraj, *Eur. J. Med. Chem.* **2011**, *46*, 3376.

[48] J. K. Barton, A. T. Danishefsky, J. M. Goldberg, *J. Am. Chem. Soc.* **1984**, *106*, 2172.

[49] N. Chitrapriya, J. H. Shin, I. H. Hwang, Y. Kim, C. Kim, S. K. Kim, *RSC Adv.* **2015**, *5*, 68067.

[50] a) S. L. Neidleman, J. L. Geigert, *Biohalogenation*, Ellis Horwood Ltd. Press, New York **1986**. b) G. J. Colpas, B. J. Hamstra, J. W. Kampf, V. L. Pecoraro, *J. Am. Chem. Soc.* **1994**, *116*, 3627.

SUPPORTING INFORMATION

Additional Supporting Information may be found online in the supporting information tab for this article.

How to cite this article: Neelakantan MA, Balakrishnan C, Selvarani V, Theetharappan M. DNA/BSA binding interactions and VHPO mimicking potential of vanadium(IV) complexes: Synthesis, structural characterization and DFT studies. *Appl Organometal Chem*. 2017;e4125. https://doi.org/10.1002/aoc.4125